P O L S K A   A K A D E M I A   N A U K

I N S T Y T U T   M A S Z Y N   P R Z E P Ł Y W O W Y C H

PRACE
INSTYTUTU MASZYN
PRZEPŁYWOWYCH

TRANSACTIONS
OF THE INSTITUTE OF FLUID-FLOW MACHINERY

95

WYDAWNICTWO IMP PAN

GDAŃSK 1993

PRACE INSTYTUTU MASZYN PRZEPŁYWOWYCH

poświęcone są publikacjom naukowym z zakresu teorii i badań doświadczalnych w dziedzinie mechaniki i termodynamiki przepływów, ze szczególnym uwzględnieniem problematyki maszyn przepływowych

*

THE TRANSACTIONS OF THE INSTITUTE OF FLUID-FLOW MACHINERY

exist for the publication of theoretical and experimental investigations of all aspects of the mechanics and thermodynamics of fluid-flow with special reference to fluid-flow machines

REDAKCJA – EDITORIAL OFFICE

Wydawnictwo Instytutu Maszyn Przepływowych
Polskiej Akademii Nauk
ul. Gen. Józefa Fiszera 14, 80-952 Gdańsk, skr. poczt. 621,
tel. (0-58) 41-12-71 wew. 141, fax: (0-58) 41-61-44,
e-mail: tjan@imppan.imp.pg.gda.pl

ISBN 83-01-93121-1
ISSN 0079-3205

PRACE INSTYTUTU MASZYN PRZEPŁYWOWYCH

1993 Zeszyt 95

ANATOL JAWOREK [1]

Ring Probes for the Measurement of Charge on a Single Airborne Particle.

The paper concerns an electrostatic method for measuring the charge carried by a single particle of charged aerosol. The probe is in the form of a ring or a long tube. A charged particle flows throughout the interior of this ring along its axis. The voltage signal induced in a measuring circuit is a measure of the particle charge. The theoretical limit of the charge measured, determined by the thermal noise, is not lower than about $10^{-14}C$ with an inaccuracy 5%.

1. Introduction

The need to know the magnitude of charge on a single aerosol particle arises in many fields of electrostatics, for example in investigations of electrodynamic spraying, electrostatic copying or printing, electrostatic precipitation, and atmospheric research. The measurement of a charge distribution in a sample of an aerosol presents still a problem. Among the numerous methods for airborne particle charge measurements, only inductive [1-6] and contact [7-9] probes allow the measurement of charge *in situ*, and in real time.

The contact probe is made in the form of a collector of arbitrary shape, on which charged particles are captured. The impacting particles are discharged, generating voltage signals in a measuring circuit. The contact probes in the form of two coaxial cylinders and two concentric spheres were described extensively by Krupa and Jaworek [7-9].

The inductive probes do not collect the particles but only are sensitive to the charge induced on the surface of a conducting measuring electrode. This type of a probe has found wide applications in measurement of charged particles and has a numerous literature, for example [1-6], but because of the complex distribution

[1] Zakład Dynamiki Plazmy, Instytut Maszyn Przepływowych PAN, Gdańsk

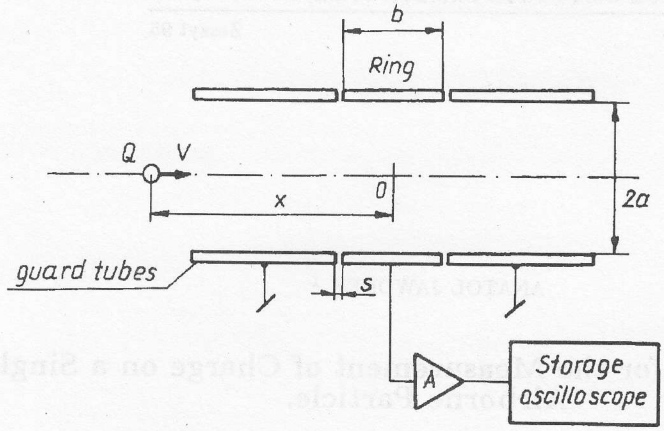

Fig. 1. Schematic diagram of the ring probe and the measuring circuit

of the electric field, the signals generated on it have hitherto not been determined in general case.

This type of a probe has been for example used by Vercoulen et al. [6] for the measurement of charges down to 10^{-16}C. This lower limit seems however to be too low, and results from the erroneous theory. As has been proved in Section 4 the lower measuring limit is determined by the noise level generated by an input resistance, and can not be decreased below the theoretical value of about 10^{-14}C without special statistical analysis, as done by Rossner and Singer [4].

The probe under consideration (Fig. 1) is made in the form of a ring or a long tube, with two co-linear guard cylinders on its both ends. The guard cylinders are not necessary. They only allow to make the analysis easier, because the measuring electrode can be regarded as a section of an infinitely long cylinder. If the guard cylinders are not used the probe characteristic ought to be determined experimentally. The inlet cylinder, which is sufficiently long, is ended with a plate in which, concentrically with the cylinder axis, a small circular aperture is made. A charged particle enters through the small aperture, and flows throughout the inner zone of these cylinders, along or near to their axis. The measuring electrode is also shielded by another metal cylinder (not shown in the figure for simplicity) which is electrically grounded.

The paper is aimed at the study of analytical parameters of the ring probes such as time domain response, frequency response, sensitivity, charge measuring limit etc.

The signals generated in the probe were measured in the circuit shown in Fig. 1. A separating amplifier is made of an electrometer valve. The potential generated in the measuring circuit or current forced by this potential and flowing to the ring can be the measure of the charge on the particle. In the present experiment the potential is measured because it allows to decrease the lower measuring limit. The signal generated by each particle is recorded by a storage oscilloscope.

The method has been verified by many authors and also in this paper. The charges measured by this method have been compared with results obtained using the Faraday cage, as a reference method.

2. Time domain response

The differential equation for the voltage $u(t)$ at the input of the measuring amplifier is:

$$-\frac{dQ_i}{dt} = C\frac{du(t)}{dt} + \frac{u(t)}{R}, \tag{1}$$

where R, C are the resistance and the capacitance at the input of the measuring circuit, and Q_i is the charge induced on the central measuring electrode. The capacitance C is the sum of the input capacitance of the measuring amplifier, the self capacitance of the probe, the capacitance of the connecting cable, and the stray capacitance. The resistance R consists of the input resistance of the measuring amplifier and the connected parallel discrete resistor.

The first term on the right hand side of Eq. (1) is the current charging the capacitance C, while the second describes the current which leaks away via the resistance R.

The general solution of the differential equation (1) is:

$$u(t) = \exp(\frac{-t}{RC}) * \int_{-\infty}^{t} \frac{1}{C}\frac{dQ_i}{dt}\exp(\frac{\theta}{RC})d\theta\,. \tag{2}$$

The voltage waveforms can be obtained from numerical calculations of Eq. (2). Because of the complex field distribution inside the cylinders and the finite length of the spacings between the measuring electrode and the guard rings the charge Q_i induced on the measuring electrode can not be determined exactly, specifically when the particle is not a point charge. For the most simple geometry presented in Fig. 1, with infinitely long guard electrodes, the charge induced on the measuring electrode by a point charge can be calculated from the surface charge density as given by the approximate relation of MacLatchy and Chipman [5]:

$$Q_i = -\frac{Q}{2}\left[\frac{vt+b/2}{(a^2+(vt+b/2)^2)^{1/2}} - \frac{vt-b/2}{(a^2+(vt-b/2)^2)^{1/2}}\right], \tag{3}$$

where Q is the particle diameter, a the internal radius of the ring, b – length of the ring, and v – the particle velocity. The time is measured in such a way that $t = 0$ when the particle is in the half of the length of the measuring electrode.

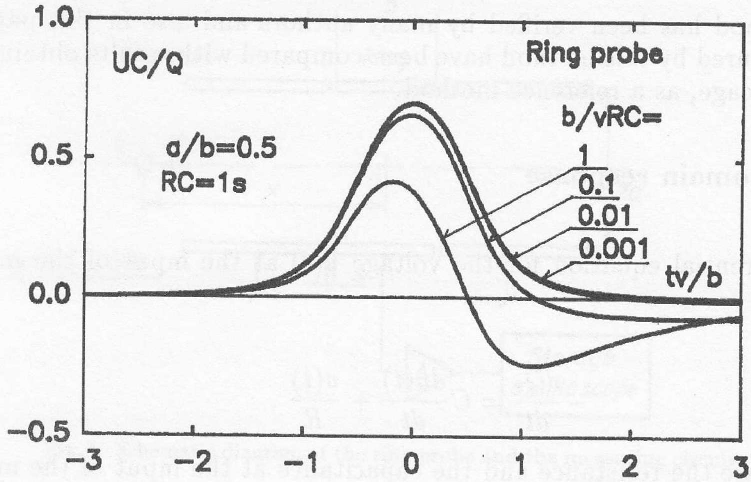

Fig. 2. Response signal of the ring probe ($a/b = 0.5$)

The general solution of the differential equation (1), with the charge Q_i given by (3), is:

$$u(t) = \frac{Qva^2}{2C}\exp(\frac{-t}{RC})*$$

$$\int_{-\infty}^{t}\left[(a^2+(v\theta+b/2)^2)^{-3/2}-(a^2+(v\theta-b/2)^2)^{-3/2}\right]\exp(\frac{\theta}{RC})d\theta\,. \tag{4}$$

Numerical solution of Eq. (4) gives the signal waveform. A series of waveforms for different $b/(vRC)$ values is plotted in Fig. 2 for a ring of a small diameter, and in Fig. 3 for a ring of a large diameter compared to its length b. The time t is normalized to b/v, so called characteristic time. The calculations are only approximate, because the effect of a radial position of the particle on the signal waveform is not considered.

Only if the time constant RC of the discharge of the capacitance C is much longer than the time during which the particle flows throughout the cylinder, i.e.:

$$\frac{b}{vCR} < 0.01 \tag{5}$$

the undershoot of the trailing edge below the base line (zero voltage axis) is negligible. If the requirement (5) is fulfilled the amplitude of the signal measured is

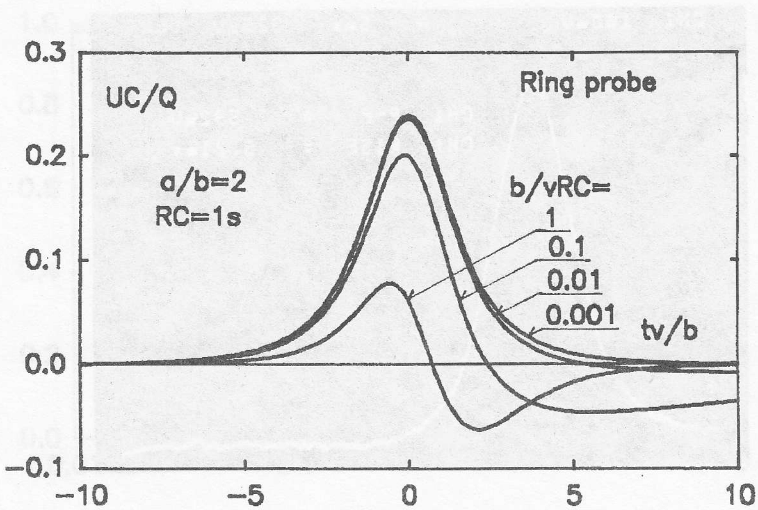

Fig. 3. Response signal of the ring probe ($a/b = 2$)

approximately independent of the particle velocity. In this case the signal attains its maximum value at $t = 0$ and equals:

$$U_m = \frac{Q}{C}\frac{b}{(4a^2 + b^2)^{1/2}} . \tag{6}$$

The results of the calculation have been compared with oscilloscope recordings such as, for example, that shown in Fig. 4. The measured signal amplitude U_m is higher than that determined from Eq. (6). This is probably caused by the edge effects i.e. it results from the finite value of the spacings s (Fig. 1) and fringing field between the particle and the measuring electrode, not taken into account in the considerations. We have observed that the signal amplitude U_m has been higher than that resulting from Eq. (6) when in preliminary experiments the spacings s were about 1.5 mm. When the spacings s where made smaller, down to about 0.5 mm, the amplitude becomes closer to the value given by Eq. (6). However, the systematic measurements have not been done. The effect of the spacing s on the generated voltage is conspicuous particularly for high a/b values.

The reduction of the signal amplitude as a function of a/b values, obtained numerically from Eq. (4) for different $b/(vRC)$ values is presented in Fig. 5, in dimensionless form. The points refer to the measurement results obtained for four different probes. They lie slightly above the theoretical curve.

For example, in order to satisfy the condition (5) with the ring of length 20 mm, and the electrical parameters of the measuring circuit $R = 10^{10}\Omega$, and $C = 100\,pF$, the particle velocity ought to be greater than $2\,m/s$.

Short probes or probes without the guard cylinders have to be calibrated, or the charge has to be calculated from Eq. (4). An example of a calibrating curve

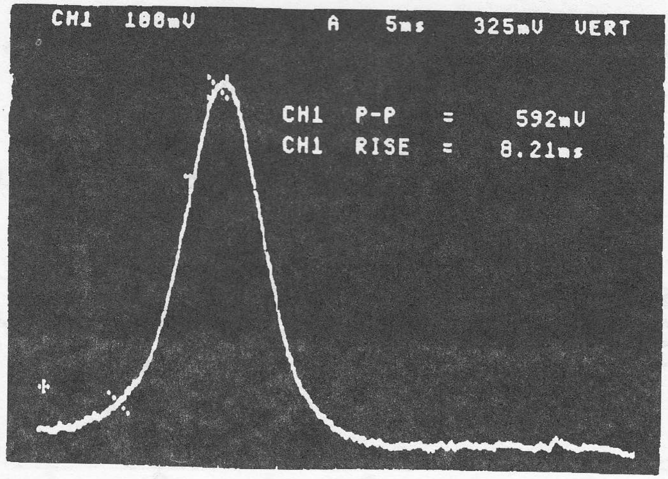

Fig. 4. Oscilloscope recording of the response signal of the ring probe ($2a = 27mm, R = 10^{10}\Omega, v = 2.5m/s, C = 317pF$)

for two probes of $a/b = 2$ and 0.5 is plotted in Fig. 6. The particle charge has been measured by means of Faraday cage as an reference method. The particle velocity has been estimated from the signal duration taken from the oscilloscope recordings. The charged droplets dripping from a metal capillary maintained at high potential were used as the test particles. Their diameters changed from $3\,mm$ down to $1\,mm$ with the voltage ranging from $50\,V$ up to $8\,kV$ respectively.

3. Measuring amplifier

In order to determine the bandwidth of a measuring amplifier the spectral density of the generated signal ought to be calculated. Too narrow bandwidth of the amplifier causes a signal amplitude suppression while too wide bandwidth causes that the rms value of the noise increases that confines the lower measuring limit. In the following considerations it is assumed that the waveforms of the measuring signal determined theoretically do not differ in the shape from that measured except of a scaling constant coefficient. It is also assumed that a particle flows along the electrode axis, and its charge is concentrated in a geometrical point.

The Fourier transform of the signal at the input of the amplifier is given by the following equation:

$$\overline{U}(j\omega) = \frac{-Q}{2C}\frac{(vRC)}{b}\left(\frac{a}{b}\right)^2 \int_{-\infty}^{+\infty} \exp\left(\frac{-t}{RC}\right) \exp\left(-j\omega t\right) *$$

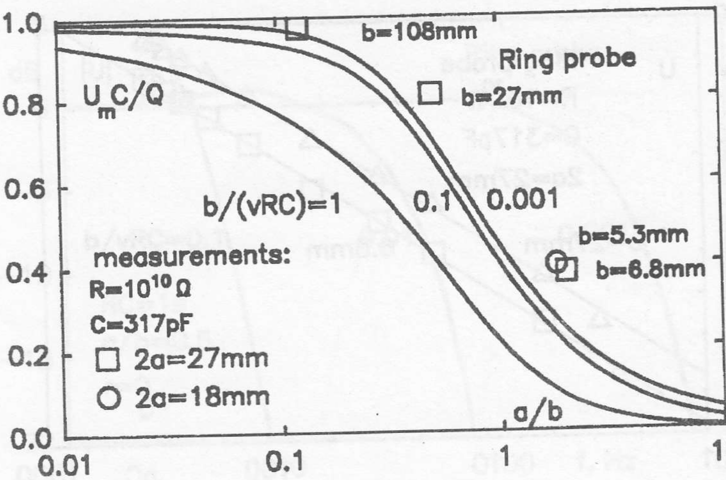

Fig. 5. Signal amplitude as a function a a/b ratio

$$\int_{-\infty}^{t}\left[\left(\left(\frac{a}{b}\right)^2+\left(\frac{v\tau}{b}+\frac{1}{2}\right)^2\right)^{-3/2}-\left(\left(\frac{a}{b}\right)^2+\left(\frac{v\tau}{b}-\frac{1}{2}\right)^2\right)^{-3/2}\right]\exp\left(\frac{\tau}{RC}\right)d\tau dt\,. \quad (7)$$

The absolute value of $|\overline{U}(j\omega)|$ represents the spectral distribution of the intensity of the signal, and is plotted in Fig. 7 (for $a/b = 0.5$) and Fig. 8 (for $a/b = 2$), for different $b/(vRC)$ values. The time constant RC was assumed to be equal $1s$. The higher the particle velocity, the wider the signal spectrum density.

To determine the signal at the output of the amplifier, let us assume that the transfer function of the measuring amplifier is in the form:

$$A(s) = A_o\frac{\omega_o}{s+\omega_o}\,, \quad (8)$$

where ω_o is the cutoff frequency of the amplifier and A_o its dc voltage gain, and the impulse response of the amplifier in the time domain:

$$h(\tau) = A_o\omega_o\exp(-\omega_o\tau)\,, \quad (9)$$

The convolution of the two functions: the impulse response (9) and the measuring signal generated in the measuring electrode (4), gives the time domain response of the amplifier. The voltage at the output of the amplifier is:

$$u_0(t) = \frac{-Q}{2C}\frac{(vRC)}{b}\left(\frac{a}{b}\right)^2\int_{-\infty}^{t}\exp\left(\frac{-\tau}{RC}\right)\exp\left(-\omega_0(t-\tau)\right) *$$

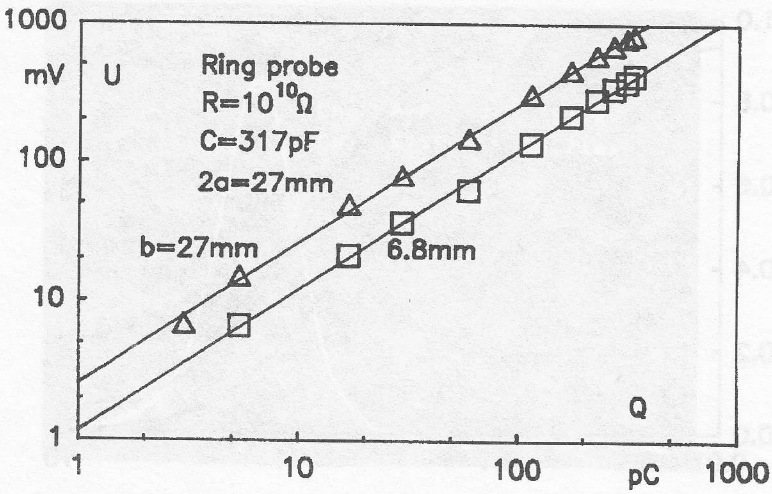

Fig. 6. Calibrating curve of the ring probes

$$\int_{-\infty}^{T}\left[\left((\frac{a}{b})^2+(\frac{v\theta}{b}+\frac{1}{2})^2\right)^{-3/2}-\left((\frac{a}{b})^2+(\frac{v\theta}{b}-\frac{1}{2})^2\right)^{-3/2}\right]\exp(\frac{\theta}{RC})d\theta dt\,.$$

The attenuation, S, of the amplitude of the output signal due to the bandwi of the amplifier is defined by the relation:

$$S=\frac{U_o}{A_o U_m}\,,$$

where: U_o is the amplitude of the signal $u_o(t)$ at the output of the ampli calculated from Eq. (10), U_m – the amplitude of the input voltage. It fol from Eq. (11) (Fig. 9) that if the cut-off frequency of the amplifier nearly equ to the 3 dB bandwidth of the signal spectrum, the pulse amplitude at the out of the amplifier is reduced nearly to about 0.75, for both probes. To obtain reduction of the amplitude to $S = 0.98$ the minimum cut-off frequency of amplifier ought to be about 140 Hz for the probe of $a/b = 0.5$ and 65 H $a/b = 2$, and $b/(vRC) = 0.01$, in both cases. The required bandwidth incre rapidly with the $b/(vRC)$ increasing.

4. Noise Characteristics

The detection of the parameters of a singular signal considerably differs fr the measurements of d.c. voltages, and even from the periodic signals. At signal levels some difficulties arise in distinguishing them from the noise. Fil tion by low-pass filters of high time constant to remove noise from *d.c.* volta

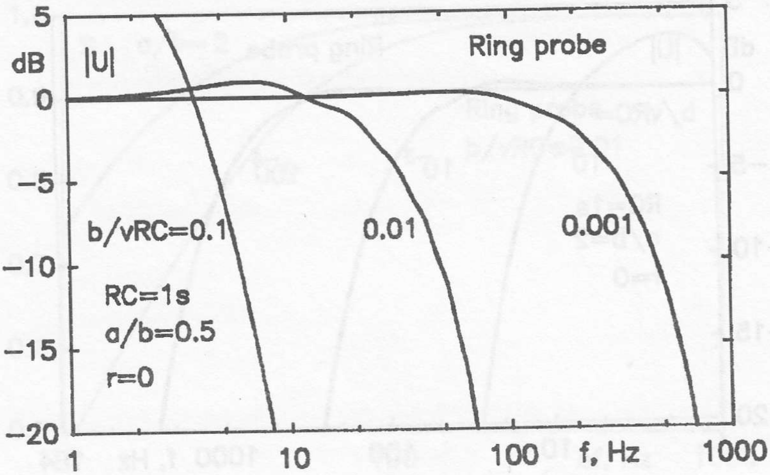

Fig. 7. Frequency response of the ring probe ($a/b = 0.5$)

or band-pass filters or phase sensitive detectors used to reduce the noise in periodic signals can not be applied in the case of a singular signal detection. The lower limit in the measurement of a particle charge is mainly confined by noise. In this section only the thermal noise generated by the input resistance R, and the equivalent noise generated by a measuring amplifier will be considered. These considerations predict the lower theoretical limit of the charge that can be measured by a ring probe. The noise caused by electromagnetic fields are not taken into account, because they can be removed by screening and grounding. Also the flicker noise of the resistor used is excluded from the considerations.

It is not possible in general case to give an exact expression for the noise voltage generated by an amplifier, because it depends on the type of the amplifier applied [10]. However, it must be remembered that the noise generated by bipolar transistors can exceed by an order or two of magnitude the noise generated by an resistor of high resistance, specifically at low frequencies. MOS, MIS and CMOS transistors are better, but the noise voltage can also exceed the value generated by the input resistance R.

The schematic diagram of the measurement circuit with an operational amplifier including the equivalent noise generators are presented in Fig. 10a. The source of the measured signal is represented by the current generator I. Voltage generator e_n is the source of the thermally generated noise by the resistance R. Noise generated by an amplifier is represented by two equivalent sources i_n and e_n.

The rms voltage of the noise generated by the resistance R in the frequency bandwidth df is given by the following equation:

$$\overline{e}_n^2 = 4kT\,Rdf \;, \tag{12}$$

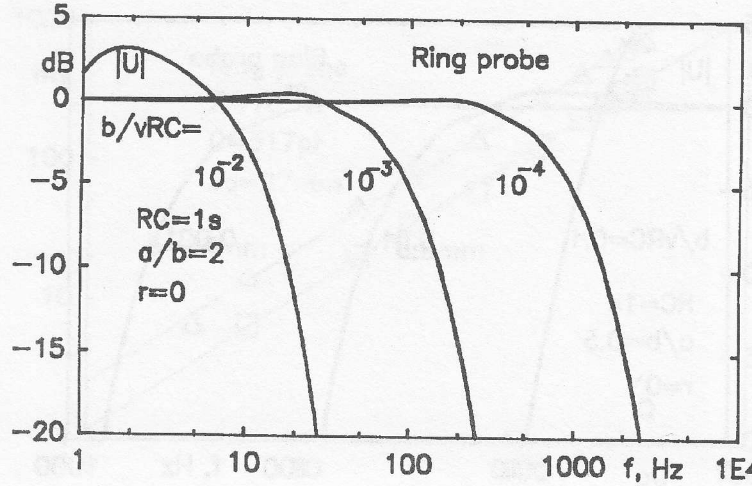

Fig. 8. Frequency response of the ring probe ($a/b = 2$)

where T is the absolute temperature, k is Boltzmann constant.

The noise voltage at the input of the amplifier generated by the source $\overline{e}$ attenuated by the RC circuit, and equals:

$$\overline{u}^2_{n1} = \int_0^{\Delta f} \frac{4kTR}{1+(2\pi f RC)^2} df = \frac{2kT}{\pi C} arctg(2\pi \Delta f RC) \, ,$$

where Δf is the bandwidth of the amplifier.

The noise voltage and noise current generated by an amplifier can be deter ned only experimentally [10]. In most practical cases they can be approxima by the following relations:

$$\overline{v}^2_n(f) = \overline{v}^2_{ns} + \overline{v}^2_{nf} \frac{f_{nv}}{f} \, ,$$

$$\overline{i}^2_n(f) = \overline{i}^2_{ns} + \overline{i}^2_{nf} \frac{f_{ni}}{f} \, ,$$

where: $\overline{v}^2_{ns}$ and $\overline{i}^2_{ns}$ are the white noise components, and $\overline{v}^2_{nf}$ and $\overline{i}^2_{nf}$ are the flic noise components at a given frequency f_{nv} and f_{ni}, respectively, (for example $1 Hz$). The spectral density of the white noise is constant over the frequency ra f_{n1} and f_{n2}. Unlike the white noise components, the flicker noise compone increase with a decreasing frequency according to $1/f$ relation down to ab $f = 10^{-6}\ Hz$ (in the case of CMOS transistors), at which it diminishes [11].

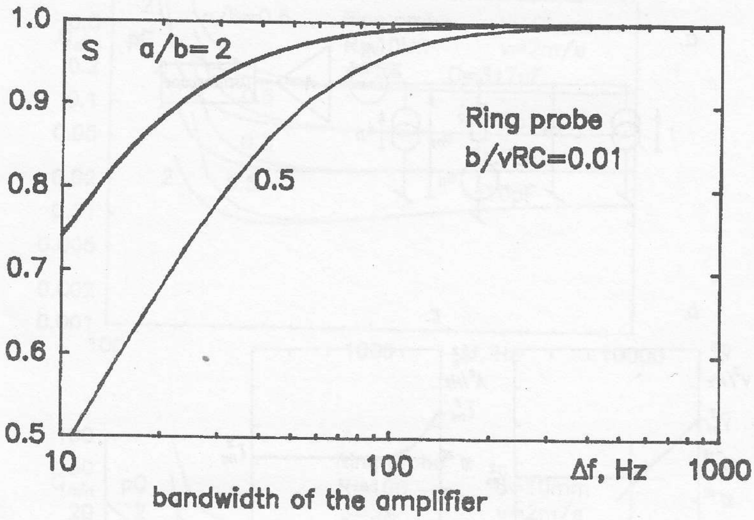

Fig. 9. Pulse amplitude attenuation at the output of the amplifier

The Equations (14) and (15) are taken from the book of Herpy [10]. The dependence of the noise voltage and of the current on the frequency are presented in Fig. 10b and c. The actual values of $\overline{v}^2_{ns}$, $\overline{i}^2_{ns}$, $\overline{v}^2_{nf}$ and $\overline{i}^2_{nf}$ can be taken from the measurements presented by the manufacturer in the data sheets.

At the input of the amplifier the voltage caused by the current noise source can be expressed as:

$$\overline{u}^2_{n2} = \int_{f_o}^{\Delta f} \frac{R^2\overline{i}^2_n(f)}{1+(2\pi fRC)^2}df =$$

$$= \frac{R\overline{i}^2_{ns}}{2\pi C}\left(arc\,tg\,(2\pi\Delta fRC) - arc\,tg\,(2\pi f_oRC)\right) +$$

$$+\frac{1}{2}R^2\overline{i}^2_{nf}f_{ni}\left(\ln\frac{(2\pi\Delta fRC)^2}{1+(2\pi\Delta fRC)^2} - \ln\frac{(2\pi f_oRC)^2}{1+(2\pi f_oRC)^2}\right), \qquad (16)$$

where f_o is the lower frequency limit of the flicker noise.

The noise generated by the voltage noise source in the bandwidth $\Delta f - f_o$ is given by the relation:

$$\overline{u}^2_{n3} = \int_{f_o}^{\Delta f}(\overline{v}^2_{ns} + \overline{v}^2_{nf}\frac{f_{nv}}{f})df = \overline{v}^2_{ns}(\Delta f - f_o) + \overline{v}^2_{nf}f_{nv}\ln\frac{\Delta f}{f_o}. \qquad (17)$$

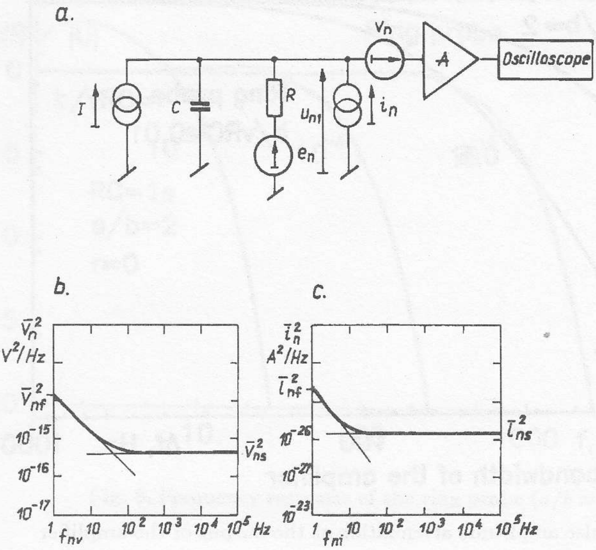

Fig. 10. Schematic diagram of the measuring circuit, including equivalent noise sources (a), the noise spectrum generated by an amplifier: voltage noise (b), current noise (c)

The effective rms value of the input noise voltage is:

$$\overline{u}_n^2 = \overline{u}_{n1}^2 + \overline{u}_{n2}^2 + \overline{u}_{n3}^2 \,.$$

The relative measuring uncertainty due to the noise is defined as the rms of the effective noise voltage related to the maximum value of the signal measured U_m:

$$\delta_n = \frac{\overline{u}_n}{U_m} \,.$$

The error caused by the bandwidth of the amplifier due to suppression of the signal amplitude is:

$$\delta_{\Delta f} = 1 - S \,.$$

The total relative measuring error δ is the sum of the error corresponding to the generated noise $\delta_n(19)$ and the error caused by the limited bandwidth of the amplifier $\delta_{\Delta f}(20)$:

$$\delta = \frac{\overline{u}_n}{U_m} + \delta_{\Delta f} \,.$$

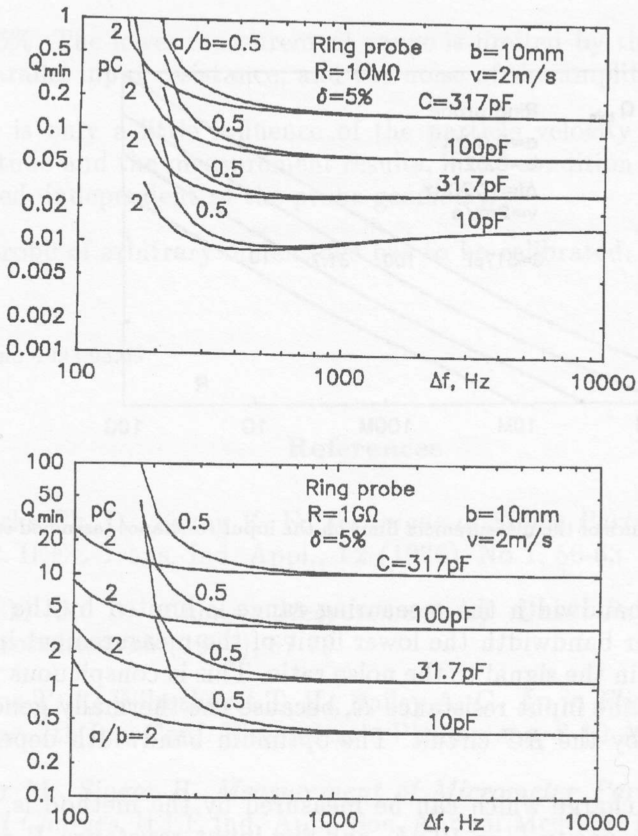

Fig. 11. Lower limit of the measurement of charge caused by the effective noise voltage and the signal suppression (the assumed error $\delta = 5\%$), $R = 10^9\Omega(a)$, $R = 10^7\Omega(b)$

In Eq. (21) the voltage U_m can be assumed to be the lowest signal amplitude measured with the total error δ. The value of the minimum charge $Q_{\min}$ measured with the error δ (the lower measuring limit) is:

$$Q_{\min}(\Delta f) = C\frac{\overline{u}_n}{\delta - \delta_{\Delta f}}, \tag{22}$$

and is plotted in Fig. 11 as the function of the bandwidth of the amplifier, and for different capacitances. The plot has been calculated for a low noise operational amplifier type LM108 with the following parameters: $\overline{v}^2_{ns} = 3*10^{-16}V^2/Hz$, $\overline{i}^2_{ns} = 2*10^{-26}A^2/Hz$, $\overline{v}^2_{nf} = 10^{-14}V^2/Hz$ at $f_{nv} = 1Hz$ and $\overline{i}^2_{nf} = 2*10^{-25}A^2/Hz$ at $f_{ni} = 1Hz$ and for $f < 10$kHz (values estimated from the plot in the book of Serpy [10]).

From the curve both the bandwidth of the amplifier and the measurement limit (the minimum charge measured with the assumed error δ) can be determined.

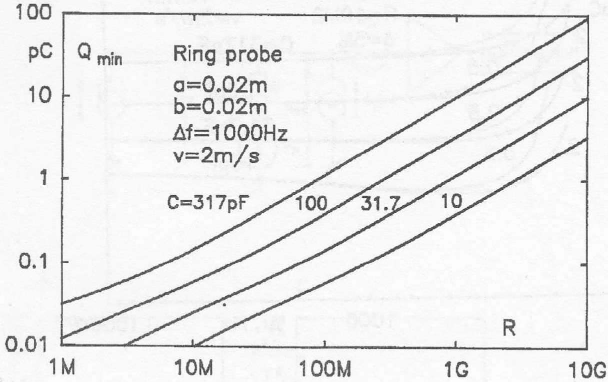

Fig. 12. The dependence of the measurement limit on the input resistance (assumed error δ – 5%

For a too narrow bandwidth the measuring range is limited by the suppre error. For the wider bandwidth the lower limit of the measurement increases cause the decrease in the signal to the noise ratio. This is conspicuous particula for lower values of the input resistance R, because the thermally generated n is not attenuated by the RC circuit. The optimum bandwidth depends also the a/b ratio.

The minimum charge which can be measured by the method is for exa $0.5\,pC$, for input capacity $C = 10\,pF$, and the input resistance $R = 1\,G\Omega$, a $0.01 pF$ for $C = 10 pF$ and $R = 10 M\Omega$. In Fig. 12 it is presented how the minim measuring range depends on the input resistance R. It should be noticed tha the resistance $R < 10 M\Omega$ the amplitude of the generated signal is of the orde $1\,mV$ or lower. It is difficult to measure the singular signals at this voltage by an oscilloscope and an a/c converter. This determines another practical li in the charge measurement. It can be concluded that the lower measuring lim the charge measurement is of the order of $10^{-14}C$, on the capacitance $C = 10$

The electromagnetic distortions (caused for example by an electrical discha or line interference ($50 Hz$) can cause the lower measuring limit to increase e by an order of magnitude.

5. Conclusions

Theoretical and experimental investigations of the measurement performa of the ring probe lead to the following conclusions:

1. The probe allows the measurement of the charge of airborne particles d to the theoretical limit not lower than about $10^{-14}C$ with an error l

than 5%. The lower measurement range is limited by the thermal noise of the parallel input resistance, and the noise of the amplifier.

2. There is only a little influence of the particle velocity upon the impulse amplitude and the measurement results, if the condition $b/(vRC) < 0.01$ is satisfied, independent of the probe geometry.

3. The probe of arbitrary dimensions has to be calibrated.

Pracę zgłoszono 1993.03.09

References

[1] Hendricks Ch. D., Yeung K. F. *Technique of Single Particle Charge Measurement.* IEEE Trans. Ind. Appl., **12** (1976), No 1, 56-63

[2] Gajewski J. B. *Charge Measurement of Dust Particle in Motion.* J.Electrostatics, **15** (1984), 67-79

[3] Williams T. J., Wilmshurst T. H., Bailey A. G. *An in Flight Particle Charge Detector.* 7th Int. Conf. Electrostatic Phenomena, 8-10 April, 1987, Oxford

[4] Rossner M., Singer H. *Measurement of Micrometer Particles by Means of Induced Charges.* IEEE Ind. Appl. Soc. Annual Meeting, 1-5 Oct., 1989, San Diego USA

[5] MacLatchy C. S., Chipman H. A. *A Dynamic Method of Measuring the Charge Induced on a Conductor.* Am. J. Phys., **58** (1990), No 9, 811-6

[6] Vercoulen P. H. W., Roos R. A., Marijnissen J. C. M., Scarlett B. *An Instrument for Measuring Electric Charge on Individual Aerosol Particles.* J. Aerosol Sci., **22** (1991), Suppl.1, 335-8

[7] Krupa A., Jaworek A. *A Method for Aerosol Particle Charge Measurements.* J. Electrostatics, **23** (1989), 283-92

[8] Jaworek A., Krupa A. *Charge Detector for Airborne Particles.* J. Electrostatics, **25** (1990), 185-99

[9] Krupa A., Jaworek A. *Sphere Probe Measuring Charge on Charged Droplets or Dust Particles.* Pom. Autom Kontr., **38** (1992), No 9, 201-3 (in Polish)

[10] Herpy M.: Analog Integrated Circuits. Akademiai Kiado, Budapest 1980

[11] Marciniak W.: Przyrządy półprzewodnikowe typu MIS. WNT, Warszawa, 1977

Sondy pierścieniowe do pomiaru ładunku pojedynczych cząstek aerozoli

Streszczenie

W artykule przedstawiono elektrostatyczną metodę pomiaru ładunku niesionego przez pojedynczą cząstkę naelektryzowanego aerozolu. Sonda wykonana jest w postaci pierścienia lub odcinka rury. Naelektryzowane cząstki przepływają wzdłuż osi rury indukując sygnał napięciowy w obwodzie pomiarowym. Dolna, wyznaczona teoretycznie granica zakresu pomiarowego ładunku na pojedynczych cząstkach aerozolu ograniczona jest szumem cieplnym i wynosi około 10^{-14} C przy błędzie 5%.